

1                   **PROBABILISTIC-BASED CHARACTERISATION OF THE MECHANICAL**  
2   **PROPERTIES OF CFRP LAMINATES**

3           S. Gomes<sup>1</sup>, D. Dias-da-Costa<sup>\*,2</sup>, L.A.C. Neves<sup>3</sup>, S.A. Hadigheh<sup>2</sup>, P. Fernandes<sup>4</sup>, E. Júlio<sup>5</sup>

4           \* corresponding author (Email: daniel.diasdacosta@sydney.edu.au)

5           <sup>1</sup>ISISE, Department of Civil Engineering, University of Coimbra, Rua Luís Reis Santos, 3030–788  
6           Coimbra, Portugal.

7           <sup>2</sup>School of Civil Engineering, The University of Sydney, Sydney, NSW 2006, Australia.

8           <sup>3</sup>Centre for Risk and Reliability Engineering, University of Nottingham, Faculty of Engineering,  
9           University Park, United Kingdom.

10          <sup>4</sup>Civil Engineering Department, Instituto Politécnico de Leiria, Portugal.

11          <sup>5</sup>CERis-ICIST, DECivil, Instituto Superior Técnico, Universidade de Lisboa, Av. Rovisco Pais,  
12          1049-001 Lisboa, Portugal

13           **Abstract**

14           Fibre reinforced polymer (FRP) composites have been increasingly used worldwide in the  
15           strengthening of civil engineering structures. As FRP becomes more common in structural  
16           strengthening, the development of probability-based limit state design codes will require accurate  
17           models for the prediction of the mechanical properties of the FRPs. Existing models, however, are  
18           based on small sample sizes and ignore the importance of the tail region for analyses and design.  
19           Addressing these limitations, this paper presents a probabilistic-based characterisation of the  
20           mechanical properties of carbon FRP (CFRP) laminates using a large batch of tension tests. The  
21           analysed specimens were pre-cured laminates of carbon fibres embedded in epoxy matrices, which  
22           is the most commonly used laminate for the strengthening concrete beams and slabs. Based on the  
23           existing data, probabilistic models and correlations were established for the Young's modulus,  
24           ultimate strain and tensile strength. Analyses demonstrate the suitability of the Weibull distribution  
25           for the estimation of CFRP properties. Results also show that the statistical characterisation of the  
26           mechanical properties should be performed with a focus on the tail region. The proposed  
27           distributions constitute a set of validated probabilistic models that can be used for performing  
28           reliability analyses of structures strengthened with CFRP laminates.

29  
30           **Keywords:** CFRP laminates; strengthening of structures; Mechanical properties; Probabilistic  
31           models.

## 32 **1. Introduction**

33 During the last decades, externally bonded reinforcement (EBR) of fibre-reinforced polymers  
34 (FRP) has become a common technique to strengthen and upgrade civil engineering structures. FRP  
35 is usually used in the form of wet lay-up sheets or pre-fabricated laminates due to their simplicity  
36 and lower capital cost. The former system is based on the direct application of fibre sheets saturated  
37 with resin, whereas the second uses pre-fabricated cured strips. There are also automated techniques  
38 using vacuum (e.g. resin infusion techniques) or vacuum and heat (e.g. heated vacuum bag only) for  
39 impregnation of fibres [1-3]. The characteristics of the FRP, namely its lightweight, high durability  
40 in aggressive environments, ease of installation and cost effectiveness, are quite competitive for  
41 strengthening purposes and constitute a good alternative to more traditional methods and materials,  
42 such as EBR using steel plates or concrete jacketing [1]. There are several examples where FRPs  
43 were used to increase the flexural, shear or axial capacity of structural members, such as beams,  
44 slabs, columns, or joints [4-8].

45 The growing interest in FRP composites resulted in the development of several design guidelines  
46 (e.g. CEB-FIB [9], TR-55 [10], CNR [11] and ACI 440.2R-08 [12]). These, however, are not  
47 presently at a level of development comparable to those used in structural concrete and steel design.  
48 Considering the uncertainties present in FRP applications, new guidelines are required to develop  
49 probability-based limit state design codes and to support the acceptance of FRP materials in civil  
50 engineering [13, 14]. Despite previous reliability studies (e.g. Ellingwood [13], Plevris,  
51 Triantafillou [15], Okeil, El-Tawil [16], Monti and Santini [17], Atadero, Lee [18], Atadero and  
52 Karbhari [19], Okeil, Belarbi [20], and Ali, Bigaud [21]) having addressed some of these  
53 uncertainties, the statistical information is still limited in the development of more accurate  
54 probabilistic models.

55 A variety of factors affect the properties of FRP after manufacturing which create a degree of  
56 uncertainty and must be considered in design [22]. Atadero [23] employed normal, log-normal,

57 Weibull and Gamma distributions to analyse the probabilistic properties of field-manufactured wet  
58 lay-up carbon and glass composites. Six sets, composed by one, three or four subsets resulting in  
59 903 samples, were considered to assess the tensile strength, the Young's modulus and the laminate  
60 thickness. Despite the large number of samples used, the need to divide them in smaller subsets of  
61 different properties and manufacturing processes led to a significant reduction in the sample size  
62 available for the statistical analysis. From this study, the Weibull distribution was proposed to  
63 model the tensile strength, whereas the Young's modulus and the laminate thickness were modelled  
64 using a log-normal distribution. Zureick, Bennett [24] performed statistical analysis on over 600  
65 samples of pultruded composite materials fabricated from E-glass fibres and polyester or vinylester  
66 matrices. However, due to the differences in the properties of the specimens, each subset contained  
67 no more than 30 samples. Zureick, Bennett [24] investigated the longitudinal tensile and  
68 compressive strengths, the longitudinal tensile and compressive modulus, the shear strength and  
69 modulus. The Weibull distribution was proposed to model the strength and stiffness properties.  
70 Further studies on the probabilistic properties of composites can be found in Jeong and Sheno [25]  
71 or Lekou and Philippidis [26].

## 72 **2. Research Significance**

73 The main limitations in previous studies are mainly related with the small size of the samples that  
74 makes it difficult to accurately characterise probabilistic distributions. Previous models focused on  
75 the entire sample distribution and ignored the importance of the tail region for probabilistic  
76 analysis. It is also difficult to obtain suitable probability distribution functions without sufficient  
77 number of samples and to output accurate estimates for the tail region. As such, discrepancy  
78 between existing models and experimental data could reach several orders of magnitude [27]. To  
79 address these limitations, the main aim of this work is to validate and propose probabilistic models  
80 for the mechanical properties of the carbon FRP (CFRP) laminates (i.e. Young's modulus, ultimate

81 strain and tensile strength) and to highlight the importance of the tail of the sample distribution. All  
82 statistical analyses are performed on a large and homogeneous batch of samples.

### 83 3. Experimental Tests

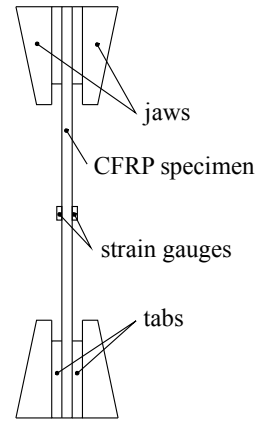
84 The data used in the present study concerns pultruded laminates produced from the same  
85 manufacturer. The CFRP had a density of  $1.4\text{g/cm}^3$  and a fibre content above 68% in volume, with  
86 a tensile design stress of 1000 MPa and 1300 MPa, respectively for 0.6% and 0.8% elongation. As  
87 part of the quality process of the manufacturer, the mechanical properties of the CFRP were  
88 consistently assessed in the fibre direction. In total, a large set of 1368 coupon samples were  
89 obtained for this process, collected from specimens with various cross sections ( $60\text{-}168\text{ mm}^2$ ) – see  
90 appendix A for complete sample characterisation.

91 The coupon configuration for tensile testing was based on the EN ISO 527-5 [28] standard  
92 (Table 1), with all the tensile tests being carried out according to same standard on a Zwick Z100  
93 universal testing machine (Figure 1a). As part of the experimental procedure, a pre-load of 0.1 kN  
94 was applied to avoid any misalignment within the system. Then, each coupon sample was loaded at  
95 a constant displacement rate of 2 mm/min until failure. Both loading and CFRP strain were directly  
96 measured using a load cell and a strain gauge, respectively (Figure 1b).

97 Table 1. Details of the tensile samples based on EN ISO 527-5 [28].

Detail	Values (mm)
FRP length	250
FRP width	15 ( $\pm 0.5$ )
FRP thickness	1.0 ( $\pm 0.2$ )
Tab extension	> 50
Tab thickness	0.5-2
Grip extension	$\geq 7$
Gauge length	50 ( $\pm 1$ )
Bevel angle	90

98



(a)

(b)

Figure 1. Experimental test set-up: (a) testing machine (courtesy of S&P Clever Reinforcement Ibérica); (b) instrumentation.

It should be denoted that the pre-load was considered in the analyses described in the following sections. Furthermore, the data for statistical analysis was carefully selected to exclude invalid results arising from: (i) tab region failure; (ii) broken fibres in contact with the strain gauge; (iii) slippage of specimens from the jaws; and (iv) failure of specimens at or close to the jaws. The stress versus strain curves were plotted, and the tensile strength, modulus of elasticity, and ultimate strain of the FRP were calculated. Figure 2 illustrates typical raw stress-strain diagrams for coupon samples tested where the linear elastic behaviour can be observed nearly up to failure.

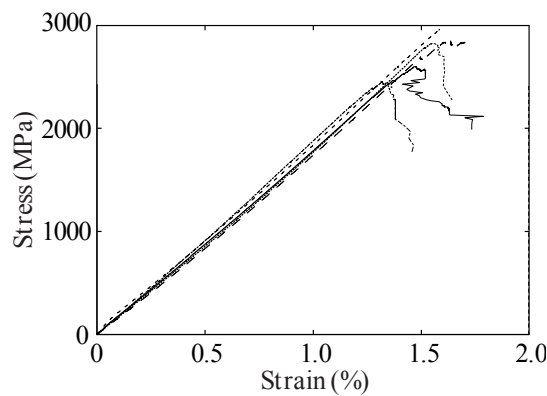


Figure 2. Raw stress-strain diagrams for five tested coupon samples.

#### 112 4. Statistical Models

113 Three statistical distributions were considered to model the CFRP properties: (i) normal; (ii) log-  
114 normal; and (iii) Weibull. The probability density function (PDF) and the cumulative distribution  
115 function (CDF) for each distribution were obtained from the following relationships.

116 - *Normal distribution*

$$117 \quad \text{PDF: } f(x|\mu, \sigma) = \frac{1}{\sigma\sqrt{2\pi}} e^{-\frac{1}{2}\left(\frac{x-\mu}{\sigma}\right)^2}, \quad \sigma > 0, -\infty < x, \mu < +\infty, \quad (1)$$

$$118 \quad \text{CDF: } F(x|\mu, \sigma) = \frac{1}{\sqrt{2\pi}} \int_{-\infty}^x e^{-\frac{1}{2}\left(\frac{t-\mu}{\sigma}\right)^2} dt, \quad (2)$$

119 where  $\mu$  is the mean and  $\sigma$  is the standard deviation, and  $t$  is a real variable.

120 - *Log-normal distribution*

$$121 \quad \text{PDF: } f(x|\mu, \sigma) = \frac{1}{x\sigma\sqrt{2\pi}} e^{-\frac{(\ln x - \mu)^2}{2\sigma^2}}, \quad x > 0, \sigma > 0, -\infty < \mu < +\infty, \quad (3)$$

$$122 \quad \text{CDF: } F(x|\mu, \sigma) = \frac{1}{\sigma\sqrt{2\pi}} \int_0^x \frac{1}{t} e^{-\frac{1}{2}\left(\frac{\ln t - \mu}{\sigma}\right)^2} dt. \quad (4)$$

123 - *Weibull distribution*

124 Since previous studies [29] showed that the statistical characterisation of the CFRP does not  
125 improve using a three-parameter Weibull distribution, a two-parameter approach was adopted here.  
126 This is defined by the following expressions:

$$127 \quad \text{PDF: } f(x|\alpha, \beta) = \frac{\alpha}{\beta} \left(\frac{x}{\beta}\right)^{\alpha-1} e^{-\left(\frac{x}{\beta}\right)^\alpha}, \quad \alpha, \beta \geq 0, 0 \leq x < +\infty, \quad (5)$$

$$128 \quad \text{CDF: } F(x|\alpha, \beta) = 1 - e^{-\left(\frac{x}{\beta}\right)^\alpha}, \quad (6)$$

129 where  $\alpha$  and  $\beta$  are the shape and the scale parameters, respectively.

130 The best-fit distributions were found following the censored maximum likelihood estimation  
 131 (MLE) [30]. This method allows estimating parameters  $\theta$  of a statistical distribution for a sample,  
 132 considering the following:

$$133 \quad L(\theta | \hat{x}_1, \hat{x}_2, \dots, \hat{x}_n) = \prod_{i=1}^n f_X(\hat{x}_i | \theta), \quad (7)$$

134 in which  $L(\cdot)$  is the likelihood that the parameters  $\theta = \theta_1, \theta_2, \dots, \theta_n$  properly describe the sample  
 135  $\hat{x} = \hat{x}_1, \hat{x}_2, \dots, \hat{x}_n$ , and  $f_X$  is the joint PDF of a sample. The maximum likelihood estimators are  
 136 computed from the set of parameters that maximise the likelihood function by considering all  
 137 possible cases of  $\theta$ .

138 Since the tail region is critical for structural reliability analysis and prediction, especial attention  
 139 is given to this region in the statistical analysis of the tensile tests. The adopted technique considers  
 140 explicitly the values of the lower tail that are smaller than a predefined bound, whereas the  
 141 remaining values are used implicitly [31]. The censored MLE can be defined as follows:

$$142 \quad L = L1 \times L2, \quad (8)$$

143 with

$$144 \quad L1 = \prod_{i=1}^j f(x_i | \theta), \quad (9)$$

$$145 \quad L2 = P(X \geq x_G | \theta)^{n-j}, \quad (10)$$

$$146 \quad P(X \geq x_G | \theta) = 1 - F(x_G | \theta), \quad (11)$$

147 where  $L1$  is the likelihood associated with the  $j$  observations of values equal or lower than the  
 148 bound value  $x_G$ .  $L2$  is the likelihood associated with the observations of values higher than the  
 149 bound value  $x_G$ .  $F(x_G | \theta)$  is the CDF of  $x_G$  given the PDF  $\theta$ ,  $n$  is the total number of

150 observations and  $n - j$  is the total number of observations exceeding the bound value  $x_G$ . The best  
 151 fit can be computed iteratively through the optimisation problem of maximising  $L$ .

152 For each property, the distributions families were adjusted for the entire sample and the lower  
 153 percentiles of: 20<sup>th</sup>, 25<sup>th</sup>, 30<sup>th</sup>, 35<sup>th</sup> and 40<sup>th</sup>. The 20<sup>th</sup> percentile is considered to be a reasonable  
 154 choice for reliability studies in this research, since it includes the region of interest without  
 155 decreasing the sample size to statistically meaningless values.

156 The goodness of fit for all distributions was examined using the Anderson-Darling test for the:  
 157 (i) entire samples; and (ii) samples with right-censored data. The Anderson-Darling test was  
 158 adopted since it provides adequate comparison tools for tail regions [32]. The statistic for the right-  
 159 censored data and entire data can be obtained respectively by [33]:

$$160 \quad A^2 = -\frac{1}{n} \sum_{i=1}^r (2i-1) [\ln Z_{(i)} - \ln(1 - Z_{(n+1-i)})] - n, \quad (12)$$

$$161 \quad A_{r,n}^2 = -\frac{1}{n} \sum_{i=1}^r (2i-1) [\ln Z_{(i)} - \ln\{1 - Z_{(i)}\}] - 2 \sum_{i=1}^r \ln\{1 - Z_{(i)}\} - \frac{1}{n} [(r-n)^2 \ln\{1 - Z_{(r)}\} - r^2 \ln Z_{(r)} + n_{(r)}^2],$$

162 (13)

163 where  $r$  is the uncensored observation,  $n$  is the total number of observations and  $Z$  denotes the  
 164 CDF of the probability distribution. The statistic values ( $A^2$ ) were then compared with the critical  
 165 values (CV) presented by Stephens and D'Agostino [33]. The null hypothesis ( $H_0$ ) of the data  
 166 following the distribution tests was not rejected if the statistic value was lower than the critical  
 167 value. The critical values for different percentiles are given in Table 2. To minimise Type I errors,  
 168 which occur when  $H_0$  was wrongly rejected, or Type II errors, in which  $H_0$  was wrongly accepted,  
 169 the significance level ( $\alpha$ ) was set at 10%.

170 Table 2. Critical values for different percentiles.

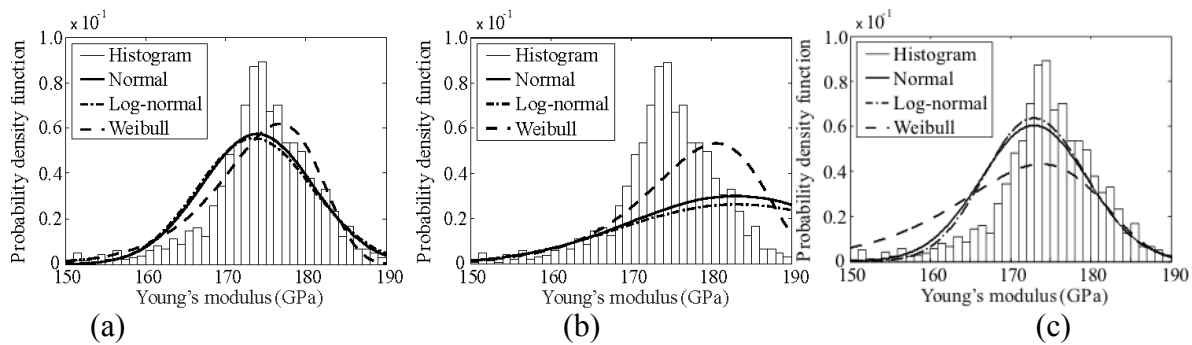
Percentile	20%	25%	30%	35%	40%	100%
CV	0.436	0.545	0.651	0.756	0.857	1.933



171 **4.1. Young's modulus**

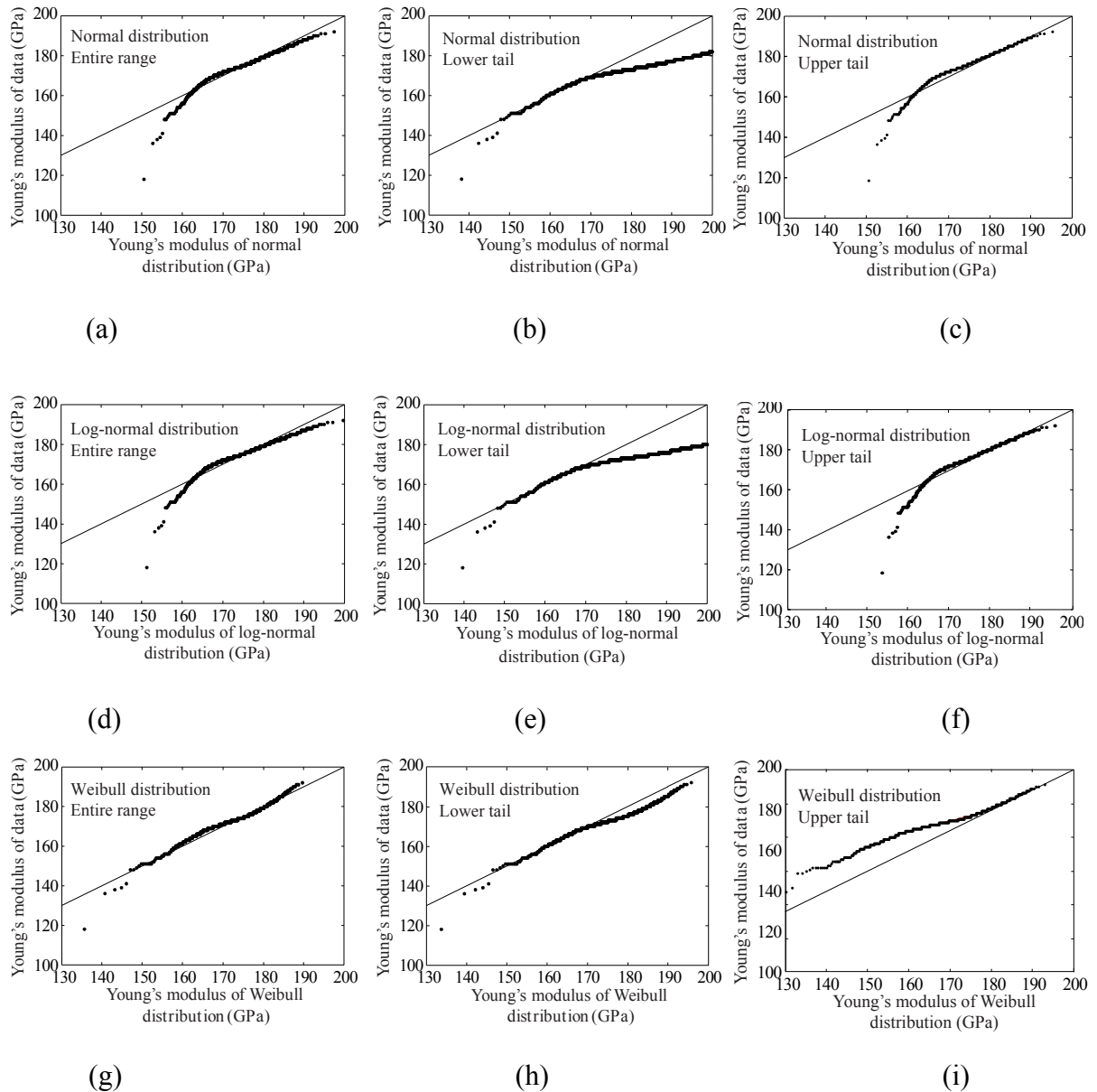
172 The Young's modulus is one of the significant parameters related with the structural safety of the  
173 FRP for rehabilitation of structures, particularly in situations where failure is expected to occur at  
174 tensile stresses significantly lower than the ultimate strength of the FRP. This type of failure usually  
175 occurs when debonding of the CFRP or concrete crushing are the dominant failure mechanisms [9].

176 The best fit for each PDF for the Young's modulus is illustrated in Figure 3. As it can be seen in  
177 Figure 3a, when the distributions were fitted to the entire sample, significant differences existed in  
178 the range of the lower and upper values. Considering the importance of the tail regions in safety  
179 assessment, clear improvements were achieved by applying the approach described above firstly to  
180 the lower 20th percentile region – see Figure 3b. Both normal and log-normal distributions provided  
181 similar results, whereas the Weibull distribution showed the closest fit to the data. For more clarity,  
182 the Q-Q curves were plotted for three distributions in Figure 4. The Weibull distribution was able to  
183 approximate the experimental data with high precision in both 20th percentile lower tail and entire  
184 range regions (Figure 4e and Figure 4f).



185  
186  
187 Figure 3. PDF for the Young's modulus of: (a) the entire data fit, (b) the 20<sup>th</sup> percentile lower tail  
188 fit; and (c) the 20<sup>th</sup> percentile upper tail fit.

189



190

191

192

193

194

195

196

197

198

199

200

201

202

203

204

Figure 4. Q-Q plot of the Young's modulus based on: normal distribution adjusted to (a) the entire range, and (b) the 20<sup>th</sup> lower and (c) 20<sup>th</sup> upper percentile; log-normal distribution adjusted to (d) the entire range, and (e) the 20<sup>th</sup> lower and (f) 20<sup>th</sup> upper percentile; and Weibull distribution adjusted to (g) the entire range, and (h) the 20<sup>th</sup> lower and (i) 20<sup>th</sup> upper percentile.

The statistic values for the Anderson-Darling goodness of fit test are presented in Table 3. In this table, the shaded cells refer to tests where the distributions were not rejected. The results showed that the Weibull was the only distribution where the null hypothesis was not rejected for the highest percentile (in this case the 25<sup>th</sup>). Additionally, this distribution presented the smallest statistical

205 values, meaning that the average squared distance between the data and the fitted distribution was  
206 also the lowest.

207 Table 3. Statistical values for the Anderson-Darling goodness of fit test for each percentile and  
208 distribution.

Percentile	Normal	Log-normal	Weibull
20%	0.279	0.373	0.123
25%	0.598	0.696	0.427
30%	1.587	1.697	1.327
35%	1.587	1.697	1.327
40%	4.226	4.351	3.767
100%	18.236	23.568	13.678

209

210 Based on the statistical analysis of the experimental data, the following shape and scale  
211 parameters were proposed to model the Young's modulus based on the Weibull distribution  
212 adjusted to the 20th percentile:

$$213 \quad E_f \sim W(26.2, 180.9) \text{ GPa.} \quad (14)$$

214 Depending on the design situation, the upper percentile of the Young's modulus might also be  
215 required. For example, in situations of debonding failure, an higher value for this material  
216 parameter can provide more conservative estimates on the capacity of the structural member. For  
217 this reason, the study described in this section was similarly applied to obtain the best fit  
218 distribution for the 20th upper percentile. Results are shown in Figs. 3 and 4, whereas the Weibull  
219 distribution adjusted to the upper tail region was given by the following equation:

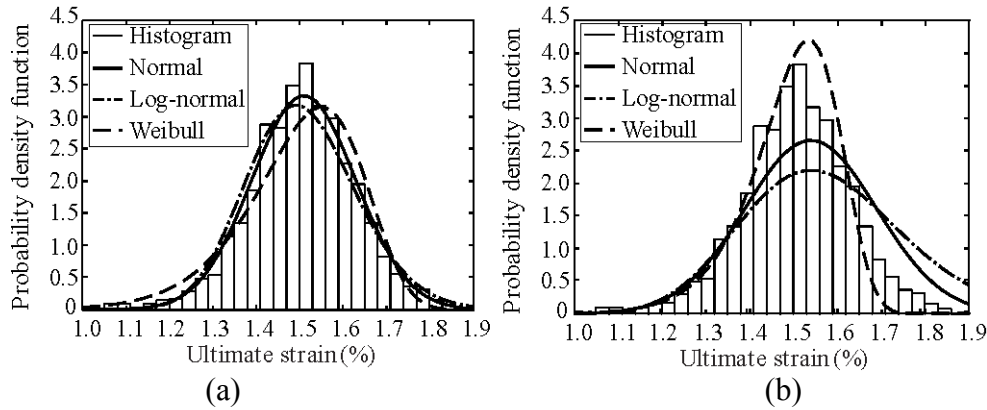
$$220 \quad E_f \sim W(20.4, 174.4) \text{ GPa.} \quad (15)$$

221 Using the distributions shown in Eqs. (14) and (15), the characteristic values for the Young's  
222 modulus were determined as 161.5 GPa and 184.0GPa, respectively corresponding to the 5th and  
223 95th percentiles. It should be mentioned that the lower value was only slightly below the design

224 value provided by the manufacturer (165 GPa). Results also showed that the coefficient of variation  
 225 was reduced, i.e., 0.04.

#### 226 4.2. Ultimate strain

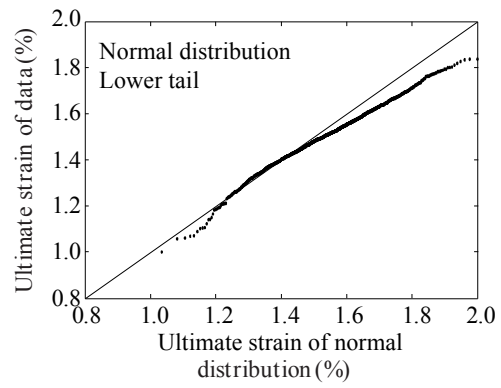
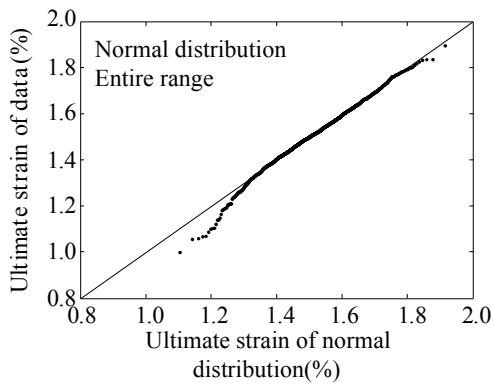
227 The ultimate strain of the FRP is another important parameter in structural safety since the  
 228 material typically exhibits elastic behaviour until failure. The same procedure described above was  
 229 followed to analyse this material parameter from the tensile tests. Conversely to what was observed  
 230 for the Young's modulus, the statistical analysis showed that (Figure 5a) none of the selected  
 231 distributions could fit well the lower tail when using the entire sample. Figure 5b shows the ultimate  
 232 strain probability density functions adjusted to the lower tail, where the Weibull distribution was the  
 233 one that provided the best results. The same trend could be seen in the corresponding Q-Q plots  
 234 illustrated in Figure 6.



235  
 236  
 237 Figure 5. PDF for the ultimate strain of the entire data fit (a) and 20<sup>th</sup> percentile lower tail fit (b).

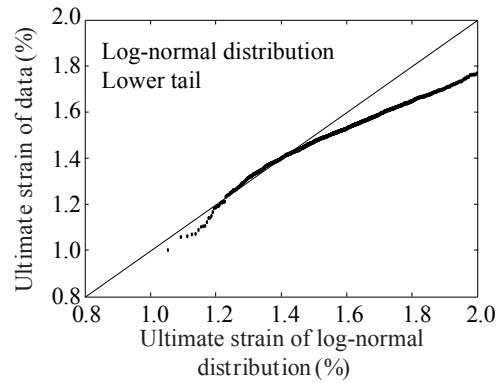
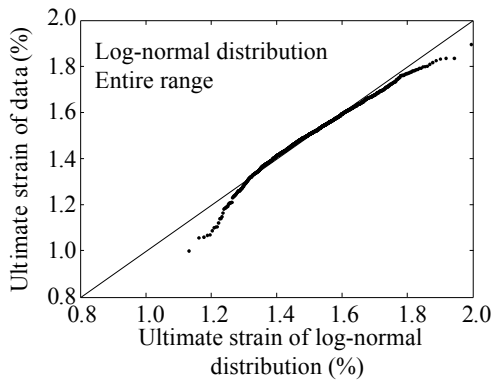
238 The Anderson-Darling goodness of fit test presented in Table 4 shows that the Weibull was the  
 239 only distribution not rejected for the highest percentile (in this case the 40<sup>th</sup>), whereas the null  
 240 hypothesis was rejected for all the distributions adjusted to the entire sample. Based on these  
 241 results, the Weibull distribution adjusted to the 20th percentile was proposed to model the ultimate  
 242 strain with a coefficient of variation of 0.06, and the following parameters:

243 
$$\varepsilon_{fu} \sim W(17.1, 1.5) \% . \tag{16}$$



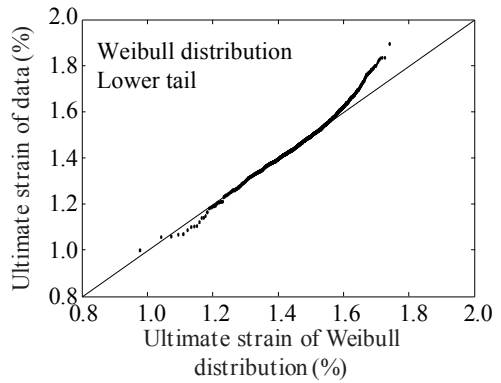
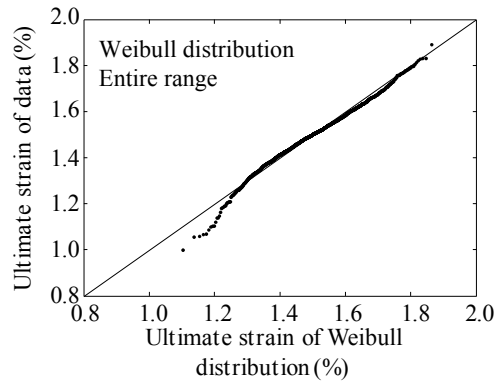
(a)

(b)



(c)

(d)



(e)

(f)

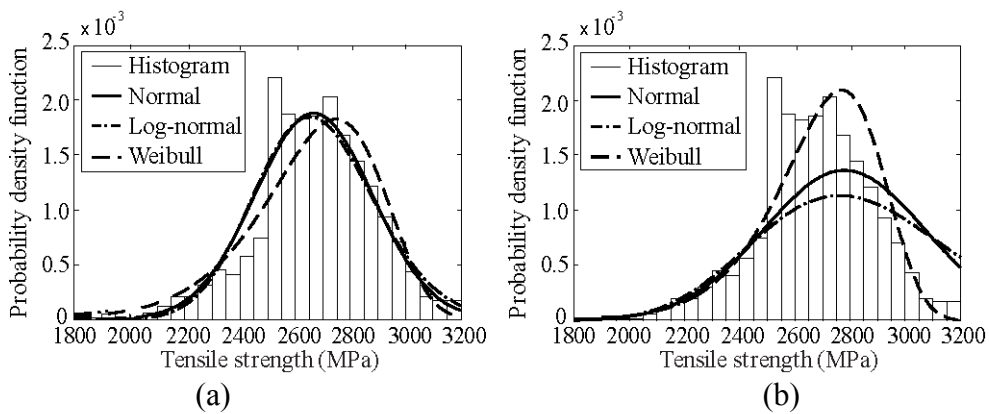
Figure 6. Q-Q plot of the ultimate strain based on: normal distribution adjusted to (a) the entire range and (b) the lower tail; log-normal distribution adjusted to (c) the entire range and (d) the 20<sup>th</sup> lower percentile; and Weibull distribution adjusted to (e) the entire range and (f) the 20<sup>th</sup> lower percentile.

255 Table 4. Statistical values for the Anderson-Darling goodness of fit test for each percentile and  
 256 distribution.

Percentile	Normal	Log-normal	Weibull
20%	0.206	0.351	0.050
25%	0.237	0.393	0.057
30%	0.433	0.656	0.101
35%	0.771	1.148	0.126
40%	1.371	2.056	0.136
100%	2.5453	5.485	8.9873

257 **4.3. Tensile strength**

258 The tensile strength of the FRP is important in situations where failure occurs within the  
 259 laminate. This can be particularly critical for prestressed FRP laminates, since the prestress loading  
 260 often represents a high percentage of the tensile strength [34, 35]. Preliminary results of the  
 261 distributions adjusted to the entire sample showed that all selected distributions were unable to  
 262 provide a good fit in the lower tail, as illustrated in Figure 7a. An improvement could be obtained  
 263 when the procedure based on fitting the CDF to the lower tail is followed – see Figure 7b. The  
 264 Weibull distribution performed better in both cases.



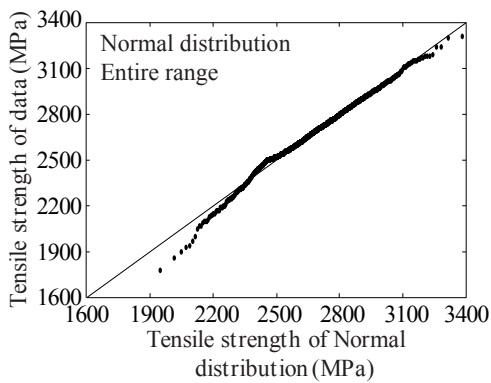
265  
 266  
 267 Figure 7. PDF for the tensile strength of (a) the entire data fit (b) and the 20<sup>th</sup> percentile lower tail  
 268 fit.

269 The Q-Q plots showed the similarity between normal and log-normal distributions – see  
 270 Figure 8a-d – and that using the entire sample was not suitable for the lower tail region. The good

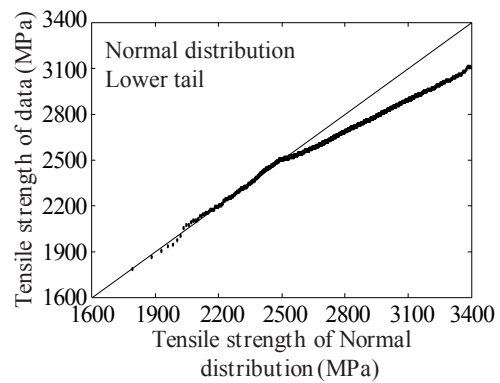
271 fit obtained with the Weibull distribution in this region can be noticed by comparing Figure 8e and  
 272 f. Despite these observations, the goodness of fit results for the lowest tail fit (Table 5) did not reject  
 273 any of the distributions for the 20<sup>th</sup> and 25<sup>th</sup> percentiles. However, since the Weibull presented a  
 274 better result than the other models overall, it was adopted here as the distribution model for the  
 275 tensile strength with the following parameters:

276  $f_f \sim W(15.9, 2777.0)$  MPa. (17)

277 The 5<sup>th</sup> characteristic value using the proposed distribution was 2304.2 MPa, which was only  
 278 0.3% higher than the experimental value (2299.0 MPa). The coefficient of variation was also very  
 279 small, i.e. 0.08. The selected distribution is in agreement with the works from Atadero [23] and  
 280 Zureick, Bennett [24] for prediction of the tensile strength based on the entire data fit.



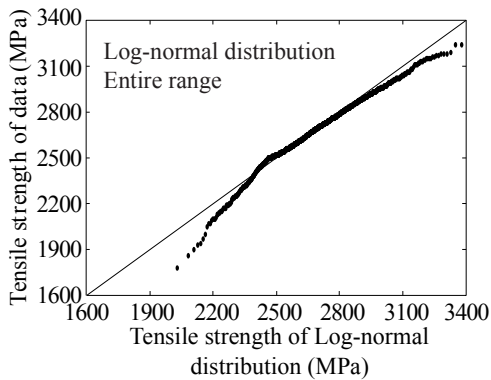
281



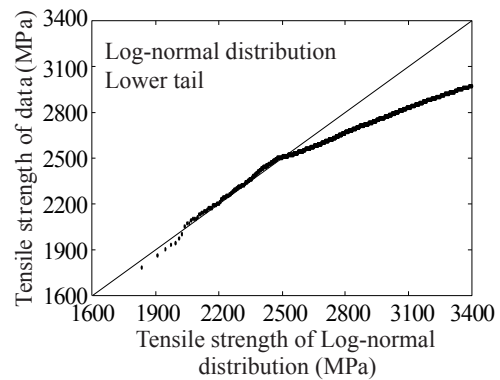
282

(a)

(b)



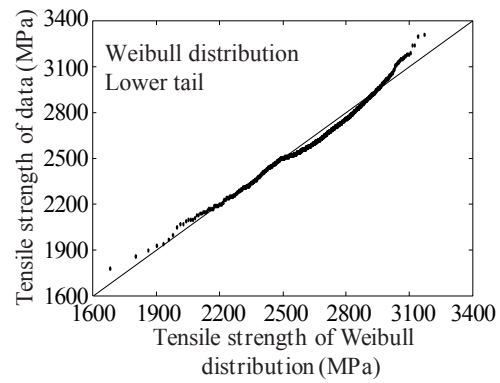
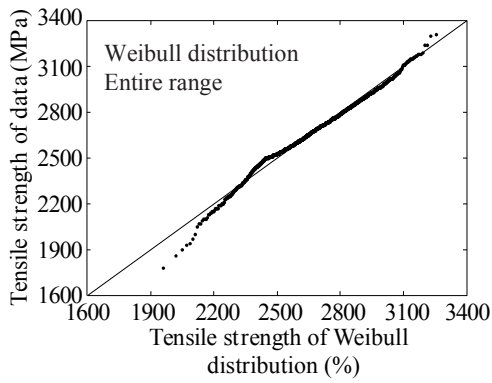
283



284

(c)

(d)



(e)

(f)

Figure 8. Q-Q plot of the tensile strength based on: normal distribution adjusted to (a) the entire range and (b) the lower tail; log-normal distribution adjusted to (c) the entire range and (d) the 20<sup>th</sup> lower percentile; and Weibull distribution adjusted to (e) the entire range and (f) the 20<sup>th</sup> lower percentile.

Table 5. Statistical values for the Anderson-Darling goodness of fit test for each percentile and distribution.

Percentile	Normal	Log-normal	Weibull
20%	0.050	0.068	0.064
25%	0.342	0.366	0.333
30%	0.894	0.941	0.817
35%	2.518	2.658	2.154
40%	4.160	4.429	3.404
100%	5.453	5.485	9.897

## 5. Correlation Analysis

This section presents a correlation analysis on the mechanical properties discussed in the previous section. Within the linear elastic range, strain, stress and Young's modulus are naturally related with each other by the Hooke's law. When approaching ultimate values – i.e. the material strength – the standard relation may no longer hold and more suitable relationships may need to be recommended for reliability analysis. The following pairs were considered: (i) tensile strength and



299 ultimate strain, (ii) tensile strength and Young's modulus, and (iii) Young's modulus and ultimate  
300 strain.

301 A linear regression analysis was firstly performed between tensile strength and ultimate strain  
302 without constraints. Results showed high correlation between these two properties ( $R^2 = 0.75$ ) as  
303 illustrated in Figure 9a. Additionally, the residual standard deviation related with the uncertainty of  
304 the proposed model was 0.062%, which means that a probabilistic model could indeed describe the  
305 correlation between the two mechanical parameters. The corresponding model was defined as  
306 follows:

$$307 \quad \varepsilon_{fu} = 0.17 + 0.0005014f_f + 0.0618Z(\%), \quad (18)$$

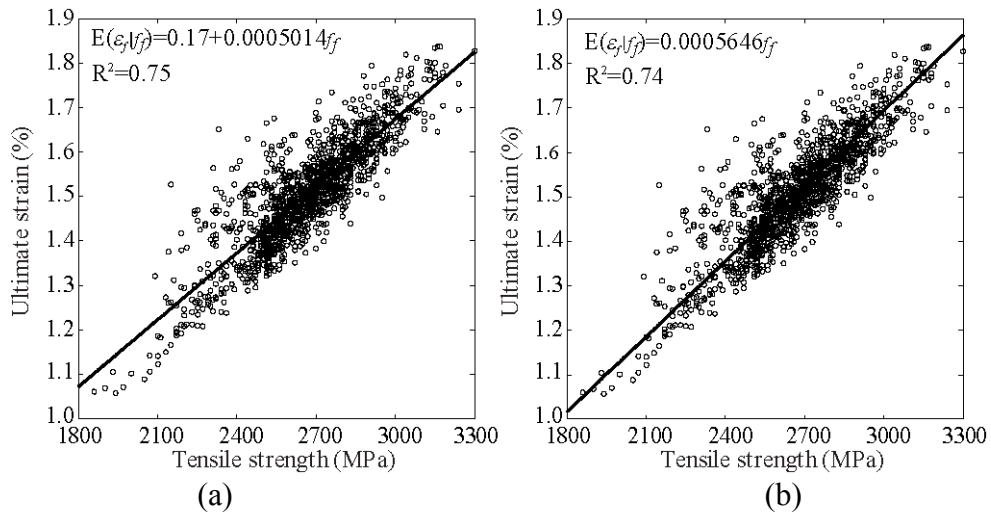
308 where  $f_f$  is the tensile strength in MPa,  $\varepsilon_{fu}$  is the ultimate strain and  $Z \sim N(0,1)$ .

309 Based on the results above, a second correlation analysis was performed by constraining the  
310 linear relation to the origin. The results and observations were quite similar, as shown in Figure 9b.  
311 The latter model had a standard deviation of 0.063% and was defined by the following expression:

$$312 \quad \varepsilon_{fu} = 0.0005646f_f + 0.0633Z(\%). \quad (19)$$

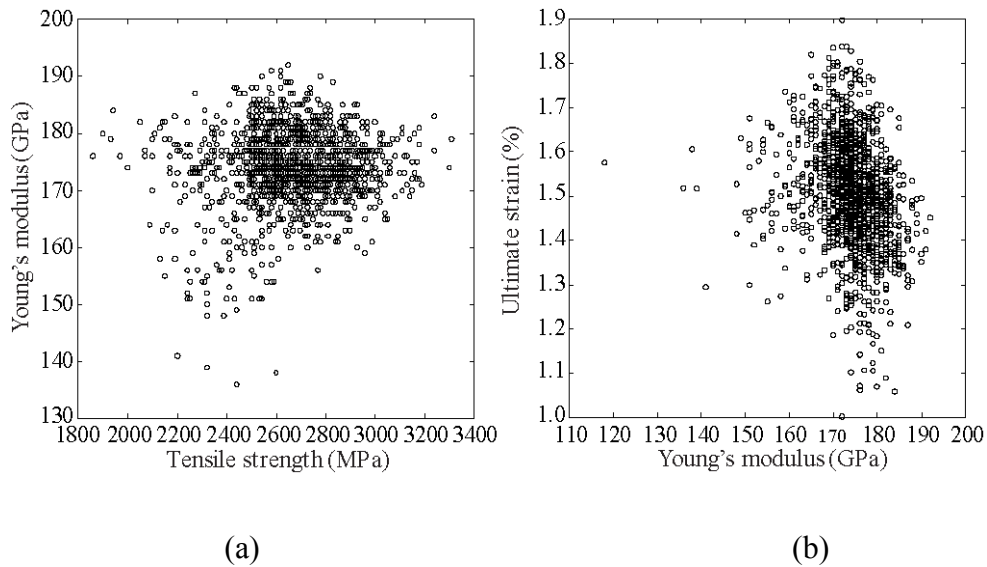
313 The last expression can be recommended in practice to relate the two expressions, since it provides  
314 good results and is relatively simple. It should be mentioned that such result shows that the ultimate  
315 strain and tensile strength are highly correlated variables. However, since both are not deterministic,  
316 the numerical value in the equation should not be directly compared with the inverse ratio of the  
317 Young's modulus – although both are similar given the linear nature of the correlation found.

318 It should be highlighted that from this study, the tensile strength and Young's modulus were  
319 found to have a small correlation – see representation in Figure 10a. Similar observation was also  
320 found between the Young's modulus and ultimate strain (Figure 10b). This suggests that the  
321 variables could be considered as independent in both situations.



322  
323

324 Figure 9. Scatter diagram of tensile strength versus ultimate strain of (a) the regression without  
325 constraints and (b) the regression across the origin.



326

327

328 Figure 10. Scatter diagram of (a) tensile strength versus Young's modulus ( $f_f$ ,  $E_f$ ) and (b)

329

Young's modulus versus ultimate strain ( $E_f$ ,  $\epsilon_{fu}$ ).

### 330 6. Conclusions

331 This manuscript presented a statistical analysis on mechanical properties of prefabricated CFRP  
332 laminates obtained from a large set of tests. Results showed that the Weibull distribution can be  
333 adopted to model the Young's modulus, the ultimate strain and the tensile strength of CFRP  
334 laminates. Furthermore, it was shown that the statistical characterisation of the CFRP should be

335 carried out giving particular attention to the tail region. In fact, although an overall good fit of any  
336 selected distribution can be achieved in most cases, the approximation obtained in the tail region is  
337 not acceptable.

338 A low variability in the mechanical properties was also observed in this study, which is most  
339 significant in terms of structural safety. The lowest coefficient of variation is found for the Young's  
340 modulus, with the characteristic values from experimental data and proposed distributions being  
341 also very similar.

342 The correlation analysis between mechanical properties demonstrated that a probabilistic model  
343 relating the tensile strength and ultimate strain can be proposed. However, despite the strain, stress  
344 and Young's modulus being related by the Hooke's law in the linear elastic region, no probabilistic  
345 model could be proposed between tensile strength or ultimate strain and Young's modulus. In fact,  
346 these pairs of variables can be considered as independent.

347 As a final note, it should be mentioned that the distributions given in this paper can be used for  
348 carrying out reliability analyses aimed at proposing partial safety factors for the future revision of  
349 design codes.

## 350 **Acknowledgements**

351 The authors acknowledge the experimental tests data provided by S&P Clever Reinforcement  
352 Ibérica. Sara Gomes would like to acknowledge the research grant from the Portuguese Science and  
353 Technology Foundation (SFRH/BD/76345/2011) and D. Dias-da-Costa would like to acknowledge  
354 the support from the Australian Research Council through its Discovery Early Career Researcher  
355 Award (DE 150101703) and from the Faculty of Engineering and Information Technologies, The  
356 University of Sydney, under the Faculty Research Cluster Program.

357 **Appendix A: sample distribution**

358 Table A-1 provides the sample size and geometrical data for the 1368 coupon samples studied in  
359 this paper.

360 Table A-1. Details of coupon samples.

Cross-section (mm <sup>2</sup> )	Area (mm <sup>2</sup> )	Sample size (#)
50×1.2	60	85
50×1.4	70	422
60×1.4	8.4	54
80×1.2	96	110
80×1.4	112	122
90×1.4	126	41
100×1.2	120	144
100×1.4	140	192
120×1.2	144	43
120×1.4	168	155

361 **References**

362 [1] Leeming MB, Hollaway LC. Strengthening of reinforced concrete structures: Woodhead Publishing  
363 Limited; 1999.

364 [2] Hadigheh SA, Gravina RJ, Setunge S. Influence of the processing techniques on the bond characteristics  
365 in externally bonded joints- Experimental and analytical investigations. *Composites for Construction*.  
366 2016;20:1-13.

367 [3] Hadigheh SA, Gravina RJ. Generalization of the interface law for different FRP processing techniques in  
368 FRP-to-concrete bonded interfaces. *Composites Part B: Engineering*. 2016;91:399-407.

369 [4] Karbhari VM. Materials considerations in FRP rehabilitation of concrete structures. *Journal of Materials*  
370 *in Civil Engineering*. 2001;13:90-7.

371 [5] Mirmiran A, Shahawy M, Samaan M, Echary HE, Mastrapa JC, Pico O. Effect of column parameters on  
372 FRP-confined concrete. *Journal of Composites for Construction*. 1998;2:175-85.

373 [6] Khalifa A, Gold WJ, Nanni A, Abdel Aziz MI. Contribution of externally bonded FRP to shear capacity  
374 of RC flexural members. *Journal of Composites for Construction*. 1998;2:195-202.

375 [7] Hadigheh SA, Gravina RJ, Setunge S. Prediction of the bond-slip law in externally laminated concrete  
376 substrates by an analytical based nonlinear approach. *Materials and Design*. 2015;66:217-26.

377 [8] Smith ST, Zhang H, Wang Z. Influence of FRP anchors on the strength and ductility of FRP-strengthened  
378 RC slabs. *Constr Build Mater*. 2013;49:998-1012.

379 [9] CEB-FIB. FIB-Bulletin 14- Externally bonded FRP reinforcement for RC structures. Geneva,  
380 Switzerland: Fédération International du Béton (FIB); 2001. p. 130.

381 [10] TR-55. Design guidance for strengthening concrete structures using fibre composite materials.  
382 SOCIETY, C.(ed.); 2000.

383 [11] CNR. Guide for the design and construction of externally bonded FRP systems for strengthening  
384 existing structures. National Research Council, Advisory Committee on Technical Recommendations for  
385 Constructuion2001.

386 [12] ACI 440.2R-08. Guide for the design and construction of externally bonded FRP system for  
387 strengthening concrete structures. Michigan (USA): MCP 2005. ACI. ; 2008.

- 388 [13] Ellingwood BR. Toward load and resistance factor design for fiber-reinforced polymer composite  
389 structures. *Journal of Structural Engineering*. 2003;129:449-58.
- 390 [14] Wang N, Ellingwood BR, Zureick AH. Reliability-based evaluation of flexural members strengthened  
391 with externally bonded fiber-reinforced polymer composites. *Journal of Structural Engineering*.  
392 2010;136:1151-60.
- 393 [15] Plevris N, Triantafillou TC, Veneziano D. Reliability of RC members strengthened with CFRP  
394 laminates. *Journal of Structural Engineering*. 1995;121:1037-44.
- 395 [16] Okeil AM, El-Tawil S, Shahawy M. Flexural reliability of reinforced concrete bridge girders  
396 strengthened with carbon fiber-reinforced polymer laminates. *Journal of Bridge Engineering*. 2002;7:290-9.
- 397 [17] Monti G, Santini S. Reliability-based calibration of partial safety coefficients for fiber-reinforced  
398 plastic. *Journal of Composites for Construction*. 2002;6:162-7.
- 399 [18] Atadero R, Lee L, Karbhari VM. Consideration of material variability in reliability analysis of FRP  
400 strengthened bridge decks. *Composite Structures*. 2005;70:430-43.
- 401 [19] Atadero RA, Karbhari VM. Calibration of resistance factors for reliability based design of externally-  
402 bonded FRP composites. *Composites Part B: Engineering*. 2008;39:665-79.
- 403 [20] Okeil AM, Belarbi A, Kuchma DA. Reliability assessment of FRP-strengthened concrete bridge girders  
404 in shear. *Journal of Composites for Construction*. 2013;17:91-100.
- 405 [21] Ali O, Bigaud D, Ferrier E. Comparative durability analysis of CFRP-strengthened RC highway  
406 bridges. *Constr Build Mater*. 2012;30:629-42.
- 407 [22] Atadero RA, Karbhari VM. Sources of uncertainty and design values for field-manufactured FRP.  
408 *Composite Structures*. 2009;89:83-93.
- 409 [23] Atadero RA. Development of load and resistance factor design for FRP strengthening of reinforced  
410 concrete structures: PhD Thesis, University of California; 2006.
- 411 [24] Zureick AH, Bennett RM, Ellingwood BR. Statistical characterization of fiber-reinforced polymer  
412 composite material properties for structural design. *Journal of Structural Engineering*. 2006;132:1320-7.
- 413 [25] Jeong HK, Sheno RA. Probabilistic strength analysis of rectangular FRP plates using Monte Carlo  
414 simulation. *Computers & Structures*. 2000;76:219-35.
- 415 [26] Lekou DJ, Philippidis TP. Mechanical property variability in FRP laminates and its effect on failure  
416 prediction. *Composites Part B: Engineering*. 2008;39:1247-56.
- 417 [27] Ellingwood BR. Acceptable risk bases for design of structures. *Progress in Structural Engineering and  
418 Materials*. 2001;3:170-9.
- 419 [28] EN ISO 527-5. Plastics- Determination of tensile properties, Part 5: Test conditions for unidirectional  
420 fibre-reinforced plastic composites. European Committee for Standardization; 2009.
- 421 [29] Alqam M, Bennett RM, Zureick AH. Three-parameter vs. two-parameter Weibull distribution for  
422 pultruded composite material properties. *Composite Structures*. 2002;58:497-503.
- 423 [30] Lindley DV. Introduction to probability and statistics. Cambridge University Press 1965.
- 424 [31] Havbro Faber M, Köhler J, Dalsgaard Sorensen J. Probabilistic modeling of graded timber material  
425 properties. *Structural Safety*. 2004;26:295-309.
- 426 [32] Lawless JF. Statistical models and methods for lifetime data: Wiley; 1982.
- 427 [33] Stephens M, D'Agostino R. Goodness-of-fit techniques: Marcel Dekker; 1986.
- 428 [34] Quantrill RJ, Hollaway LC. The flexural rehabilitation of reinforced concrete beams by the use of  
429 prestressed advanced composite plates. *Composites Science and Technology*. 1998;58:1259-75.
- 430 [35] Triantafillou TC, Deskovic N, Deuring M. Strengthening of concrete structures With prestressed fiber  
431 reinforced plastic sheets. *Structural Journal*. 1992;89:235-44.
- 432